Chem. Senses 34: 695–703, 2009 doi:10.1093/chemse/bjp056

Expression Patterns of Odorant Receptors and Response Properties of Olfactory Sensory Neurons in Aged Mice

Anderson C. Lee[1], Huikai Tian[1], Xavier Grosmaitre and Minghong Ma

Department of Neuroscience, University of Pennsylvania School of Medicine, Philadelphia, PA 19104, USA

Correspondence to be sent to: Minghong Ma, Department of Neuroscience, University of Pennsylvania School of Medicine, 215 Stemmler Hall, 3450 Hamilton Walk, Philadelphia, PA 19104, USA. email: minghong@mail.med.upenn.edu

[1]These authors contribute equally

Abstract

The sense of smell deteriorates in normal aging, but the underling mechanisms are still elusive. Here we investigated age-related alterations in expression patterns of odorant receptor (OR) genes and functional properties of olfactory sensory neurons (OSNs)—2 critical factors that define the odor detection threshold in the olfactory epithelium. Using in situ hybridization for 9 representative OR genes, we compared the cell densities of each OR in coronal nose sections at different ages (3–27 months). The cell density for different ORs peaked at different time points and a decline was observed for 6 of 9 ORs at advanced ages. Using patch clamp recordings, we then examined the odorant responses of individual OSNs coexpressing a defined OR (MOR23) and green fluorescent protein. The MOR23 neurons recorded from aged animals maintained a similar sensitivity and dynamic range in response to the cognate odorant (lyral) as those from younger mice. The results indicate that although the cell densities of OSNs expressing certain types of ORs decline at advanced ages, individual OSNs can retain their sensitivity. The implications of these findings in age-related olfactory deterioration are discussed.

Key words: aging, main olfactory epithelium, odorant responses, olfactory receptor, olfactory sensory neurons

Introduction

Decline of olfactory function is common in elderly humans, signified by an increased detection threshold and a reduced ability in odor identification and discrimination (Doty et al. 1984; Stevens and Cain 1987; Wysocki and Gilbert 1989; Ship et al. 1996; Lehrner et al. 1999; Murphy et al. 2002). Fewer studies have examined age-related smell function in other mammals, and the results differ in different olfactory tasks. Although aged animals perform some discrimination tasks just as well as their younger counterparts (Enwere et al. 2004; Joly et al. 2006), they show deficits in fine odor discrimination and a higher detection threshold (Enwere et al. 2004; Kraemer and Apfelbach 2004). Although changes centrally in the brain may contribute to the decreased sensitivity in aging, this study focuses on structural and molecular changes peripherally in the olfactory epithelium, observed in both humans (Nakashima et al. 1984; Trojanowski et al. 1991; Paik et al. 1992; Chen et al. 1993) and rodents (Hinds and McNelly 1981; Loo et al. 1996; Rosli et al. 1999; Getchell et al. 2004). The dominant changes in the aging nose include location-specific reduction of the olfactory epithelium and a net loss of sensory neurons in the affected areas (Hinds and McNelly 1981; Paik et al. 1992; Loo et al. 1996; Rosli et al. 1999), presumably due to increased cell death (Conley et al. 2003; Kern et al. 2004) and decreased neurogenesis (Loo et al. 1996; Weiler and Farbman 1997).

Odor detection critically depends on a large family (>1000 in rodents) of G-protein–coupled odorant receptors (ORs) expressed in several million olfactory sensory neurons (OSNs) harbored in the olfactory epithelium. Smell perception starts with binding of odor molecules to specific ORs, which triggers a second messenger cascade, leading to opening of specific ion channels. The subsequent depolarization of the cell membrane generates action potentials in the OSNs, which carry the odor information into the olfactory bulb in the brain (Firestein 2001; Ma 2007; Munger et al. 2009). Each OR is expressed in one of the few broad zones in the olfactory epithelium, and each OSN typically expresses one functional OR that defines its response specificity and its central target in the olfactory bulb (Mombaerts 2006).

Among the potential peripheral mechanisms, a decreased olfactory input to the brain could result from a reduced

number of OSNs expressing certain ORs and/or a reduced sensitivity of individual OSNs. To test these possibilities, we investigated age-related alterations in expression patterns of ORs and odor response properties at the single-cell level. Specifically, using in situ hybridization, we examined the expression patterns of 9 ORs in the posterior portion of the olfactory epithelium, which is subject to less environmental insults and thus better preserved in aged animals (Loo et al. 1996). The cell densities for different ORs showed differential trajectories from 3 to 27 months, and a significant decline was found for some ORs. We then compared the response sensitivity of individual OSNs expressing a defined OR from aged animals to those from younger adults. For this purpose, we used a gene-targeted MOR23 mouse line, in which all OSNs expressing the receptor MOR23 are genetically tagged by green fluorescent protein (GFP; Vassalli et al. 2002). The surface density of MOR23 cells decreased from 3 to 24 months, but the neurons from different age groups showed similar sensitivity and dynamic range in responding to lyral, the cognate ligand. These results indicate that the age-related loss of sensory neurons is not uniform among OSNs expressing different ORs and individual sensory neurons in aged mice can retain their sensitivity.

Materials and methods

Tissue preparation

Wild-type C57BL/6 mice were purchased from the Charles River Laboratories or the National Institute of Aging (NIA). Aged mice were either directly ordered from NIA or kept to the desired age in the animal facility of the University of Pennsylvania. Gene-targeted MOR23 mice (on a mixed 129 × B6 background) in which the MOR23 cells coexpress tauGFP under a bicistronic control of internal ribosome entry sites (Vassalli et al. 2002) were bred and raised in the same animal facility. All mice were kept under barrier conditions, presumably with little environmental insult. Because we did not observe systematic differences between the animals from different sources, the data obtained from the same age were grouped together.

Mice were deeply anesthetized by intraperitoneal injection of ketamine-xylazine (200–20 mg/kg body weight) before decapitation. For in situ hybridization, the heads were fixed in 4% paraformaldehyde (Sigma) overnight at 4 °C. The tissues were then decalcified in 0.5 M ethylenediaminetetraacetic acid (EDTA, pH 8.0) for up to 7 days and infiltrated in a series of sucrose solutions before being embedded in optimal cutting temperature medium (OCT). The frozen tissues were cut into 20 μm coronal sections on a cryostat. For patch clamp recordings, the heads were put into icy Ringer's solution, which contained (in mM) NaCl 124, KCl 3, $MgSO_4$ 1.3, $CaCl_2$ 2, $NaHCO_3$ 26, NaH_2PO_4 1.25, and glucose 15 (osmolarity: 305 mOsm). The pH was kept at 7.4 by bubbling with 95% O_2 and 5% CO_2. The nose was dissected out en bloc. The olfactory mucosa attached to the nasal septum and the dorsal recess was removed and kept in oxygenated Ringer's solution. Before the recording, the olfactory mucosa was peeled off from the underlying bone as a whole and transferred to a recording chamber with the mucus layer facing up, and the oxygenated Ringer's solution was continuously perfused at 25 ± 2 °C. The procedures of animal handling and tissue harvesting were approved by the institutional animal care and use committee of the University of Pennsylvania.

In situ hybridization and cell counting

Digoxigenin (DIG)-labeled RNA probes of the OR genes were generated using DIG RNA Labeling Kit (SP6/T7; Roche), and the primer sequences are included in the supplementary data (Supplementary Table 1). We initially started with ~20 randomly chosen OR genes that are expressed in different zones and then focused our analysis on 9 OR genes (Table 1). The antisense probes for these 9 ORs generated strong in situ hybridization signals. In addition, they cover different zones: 2 in the dorsomedial zone (zone 1), 2 in the intermediate zone (zones 2–3), and 5 in the ventrolateral zone (zone 4). The sections were hybridized with the RNA probes (~1 μg/ml) overnight at 65 °C in the hybridization solution (50% deionized formamide, 10 mM Tris–Cl (pH 8.0), 10% dextran sulfate, 1× Denhardt's solution, 200 μg/ml tRNA, 0.6 M NaCl, 0.25% sodium dodecyl sulfate, and 1 mM EDTA), followed by high-stringency washing steps sequentially in 2×, 0.2×, and 0.1× standard saline citrate at 65 °C (20 min in each solution). The sections were then incubated with alkaline phosphatase (AP)–conjugated anti-DIG antibody (Anti-digoxigenin-AP, Roche) at room temperature (RT) for 1 h, and the signals were detected by nitro blue tetrazolium and 5-bromo-4-chloro-3-indolyl phosphate (NBT/BCIP, Roche; 2 h at RT).

The animal numbers for different age groups are as follows: 10 (3 months), 10 (12 months), 9 (18 months), 9 (24 months), and 8 (27 months). To minimize variations from the tissue source, we only used 25–30 sections (500–600 μm) from the posterior part of the nose from each animal. These sections were collected from the presence of all turbinates to the initial appearance of the olfactory bulb with characteristic morphology shown in Figure 1A. Adjacent sections from each animal were tested for different OR probes. For each section, the cross-sectional area of the main olfactory epithelium was measured by outlining the apical surface to the lamina propria border with Canvas 9.0 software (Deneba; Figure 1A). NBT/BCIP stained cells appeared as dark brown dots in the tissue sections, and detailed counting criteria were described previously (Tian and Ma 2008b). The potential overcounting problem was not corrected (Guillery 2002) because the cell densities for all ORs were calculated and compared in the same way. Each probe was typically tested on 3 (occasionally 2 or 4) different sections per animal, and an averaged cell density

Table 1 The cell densities of 9 ORs are summarized for different ages

OR probe (other names)	Zone	Cell density (/mm^2 cross-sectional area)					*F*	*P*
		3 months	12 months	18 months	24 months	27 months		
MOR13-4 (Olfr640)	1	57.4 ± 5.7 (*n* = 6)	80.0 ± 4.6 (*n* = 6)	61.9 ± 6.4 (*n* = 6)	44.0 ± 4.3 (*n* = 6)		7.793	0.0012
MOR31-12 (Olfr648)	1	22.2 ± 1.5 (*n* = 6)	28.4 ± 3.3 (*n* = 6)	34.8 ± 3.6 (*n* = 6)	23.5 ± 2.0 (*n* = 6)		4.37	0.0160
MOR263-5 (Olfr17; P2)	2–3	58.2 ± 11.4 (*n* = 6)	74.8 ± 10.5 (*n* = 6)	87.3 ± 8.5 (*n* = 6)	84.2 ± 8.4 (*n* = 6)		1.800	0.1797
MOR279-2 (Olfr164)	2–3	23.7 ± 3.4 (*n* = 6)	34.2 ± 3.8 (*n* = 6)	32.8 ± 3.3 (*n* = 7)	19.8 ± 2.6 (*n* = 6)	11.3 ± 3.3 (*n* = 5)	7.662	0.0004
MOR0-2	4	110.7 ± 6.0 (*n* = 7)	91.7 ± 10.2 (*n* = 7)	97.4 ± 11.9 (*n* = 6)	61.2 ± 11.9 (*n* = 6)		4.251	0.0164
MOR122-1 (Olfr234)	4	41.4 ± 4.2 (*n* = 6)	50.6 ± 6.0 (*n* =6)	57.9 ± 4.6 (*n* = 6)	36.4 ± 2.3 (*n* = 6)		4.595	0.0133
MOR236-1 (Olfr1264)	4	136.0 ± 13.1 (*n* = 7)	137.5 ± 15.9 (*n* = 8)	164.4 ± 15.2 (*n* = 7)	143.2 ± 12.0 (*n* = 7)	102.4 ± 8.1 (*n* = 6)	2.438	0.0686
MOR256-3 (Olfr124; SR1)	4	128.1 ± 12.7 (*n* = 7)	120.7 ± 6.7 (*n* = 7)	135.4 ± 20.2 (*n* = 7)	113.6 ± 9.9 (*n* = 7)		0.496	0.6885
MOR267-16 (Olfr370)	4	77.9 ± 6.2 (*n* = 6)	93.6 ± 8.4 (*n* = 6)	92.0 ± 8.5 (*n* = 7)	73.2 ± 9.9 (*n* = 7)	49.1 ± 5.8 (*n* =5)	4.231	0.0090

The averaged cell density per cross-sectional area is denoted as cell number ± standard error of the mean/mm^2 (*n* = the number of animals). The *F* values and the corresponding *P* values are obtained in 1-way ANOVA tests. A significant *F* value is defined when $P < 0.05$. The statistical results for pairwise comparison are included in Figure 2.

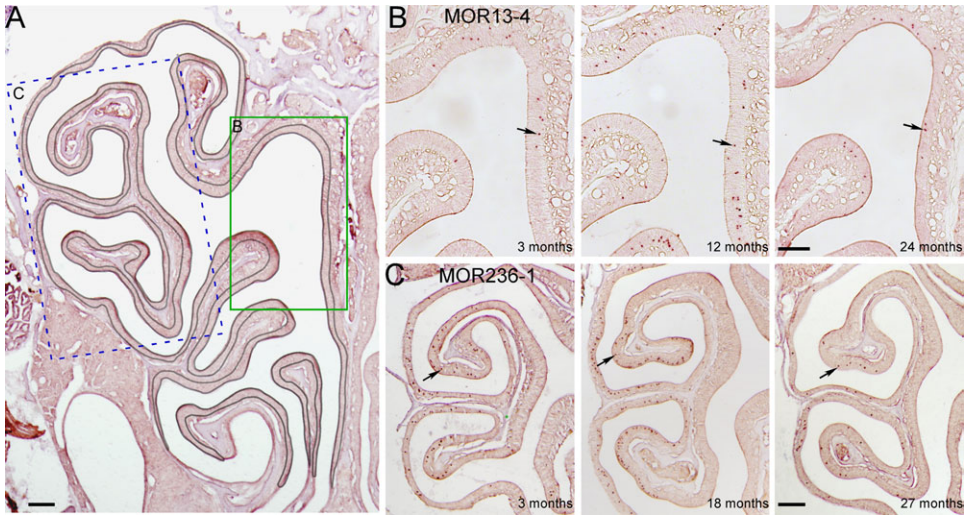

Figure 1 The densities of OSNs expressing individual OR genes are examined by in situ hybridization. **(A)** The cross-sectional area from a coronal section was determined by outlining the olfactory epithelium (the curved black line) and measuring the underneath area. This section was from an 18-month-old animal. The rectangles indicate the approximate locations from which the images in **(B, C)** were taken. **(B, C)** The coronal sections from different ages were hybridized with MOR13-4 (zone 1, **B**) and MOR236-1 (zone 4, **C**) antisense RNA probes. Arrows mark examples of labeled cells. Scale bars in **(A–C)** = 0.2 mm.

(per cross-sectional area) from these sections was obtained for that animal. Then the cell densities from different animals at the same age were averaged as mean ± standard error (*n* = the number of animals). The mean cell densities of each OR for different age groups were statistically compared using analysis of variance (ANOVA) post hoc tests in StatView 5.0 (SAS Institute). Independent ANOVA tests were performed for individual ORs. The *F* values and the corresponding *P* values generated in 1-way ANOVA tests are included in Table 1. When there is a significant *F* value, a series of pairwise comparisons are performed via post hoc tests to assess the difference between any 2 groups and the resulting

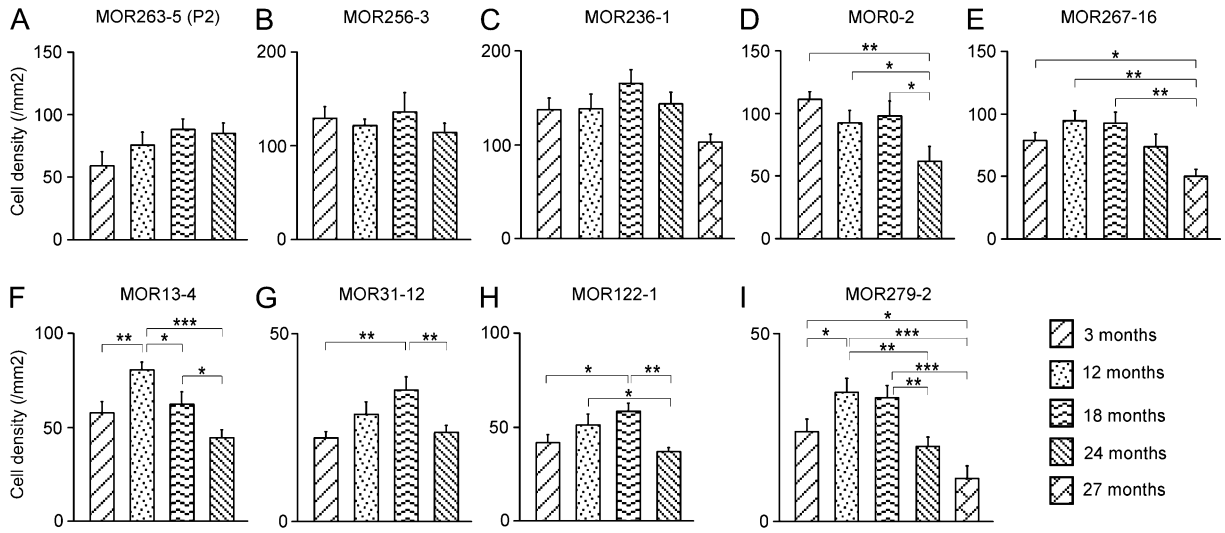

Figure 2 The densities of OSNs expressing individual OR genes show differential changes during aging. **(A–C)** There were no significant changes in the cell densities of MOR263-5 **(A)**, MOR256-3 **(B)**, and MOR236-1 **(C)**. **(D, E)** There was a significant decline in the cell densities at the last time point tested for MOR0-2 **(D)** and MOR267-16 **(E)**. **(F–I)** For these 4 ORs (MOR13-4, MOR31-12, MOR122-1, and MOR279-2), there was a significant increase in cell densities after 3 months and a significant decrease at advanced ages (24 or 27 months). For each OR, the mean cell density per cross-sectional area in mm^2 is plotted at different ages with error bars = standard errors. The pairwise comparison at different time points is obtained by ANOVA post hoc tests, and the *P* value range is marked as ***($P < 0.001$), **($0.001 < P < 0.01$), and* ($0.01 < P < 0.05$).

P values are included in Figure 2. For MOR23-GFP cells, images were taken from the whole-mount epithelium (from the septum and the dorsal recess area) using a SensiCam QE camera mounted on an Olympus BX51WI microscope with a ×40 objective. Each image covered an area of 222 μm by 168 μm, and the cell density per surface area was obtained.

Patch clamp

The dendritic knobs of the OSNs were visualized through an upright microscope (Olympus BX51WI) equipped with a CCD camera (Dage-MTI) and a ×40 water immersion objective. An extra ×4 magnification was achieved by an accessory lens in the light path. Electrophysiological recordings were controlled by an EPC-10 amplifier combined with Pulse software (HEKA Electronic). Perforated patch clamp was performed on the dendritic knobs by including 260 μM nystatin in the recording pipette, which was filled with the following solution (in mM): KCl 70, KOH 53, methanesulfonic acid 30, ethyleneglycol-bis(aminoethylether)-tetraacetic acid 5.0, *N*-2-hydroxyethylpiperazine-*N*′-2-ethanesulfonic acid 10, and sucrose 70; pH 7.2 (KOH) and 310 mOsm. The junction potential was approximately 9 mV and corrected in all experiments off-line. A multibarrel pipette, placed ~20 μm downstream from the recording site, was used to deliver odorant stimuli by pressure ejection through a Picospritzer (General Valve). Lyral (from International Flavors and Fragrances Inc.) was dissolved at 0.5 M in dimethyl sulfoxide and kept at –20 °C. The solutions with the final concentrations were diluted by adding Ringer and prepared before each experiment.

Results

Age-related changes in expression patterns of individual ORs

To investigate age-related alterations in expression patterns of ORs, we examined coronal sections from the better protected, posterior part of the nose. Sections within a narrow range (starting from the presence of all the turbinates to the initial appearance of the olfactory bulb) from each animal were used for the following reasons. First, this portion is better preserved in the aged animals (Loo et al. 1996) and the observed changes likely result from aging per se instead of age-associated conditions (such as environmental insults). Second, these coronal sections display characteristic morphology and cover all 4 zones. Third, taking the sections based on physical landmarks facilitate comparison of the data obtained from different age groups. We did not observe obvious damage to the olfactory epithelium sections we used from aged animals. The zonal distribution of OSNs stained by individual OR probes was normal without apparent disruption.

We selected 9 OR genes expressed in different epithelial zones to examine their cell densities from 3 to 24 months (to 27 months for 3 ORs) using in situ hybridization (Table 1). DIG-labeled antisense RNA probes were generated to detect the mRNA levels of individual OR genes in single OSNs. All probes detect only their target OR gene except for one probe: MOR279-2, which detects both MOR279-2 and MOR279-1 mRNAs (~90% nucleotide identity). As examples, the labeled cells by 2 probes, MOR13-4 and MOR236-1, are distributed in zone 1 and zone 4, respectively (Figure 1B,C).

The cell densities (the number of labeled cells/cross-sectional area in mm^2) for all ORs are summarized in Table 1 and Figure 2.

The expression patterns of these 9 OR genes show differential trajectories with age, and they are classified into 3 categories for the purpose of clear description. In the first category, which includes 3 ORs (MOR263-5, MOR256-3, and MOR236-1), the cell density did not significantly change from the first to the last time point tested (Figure 2A–C). In the second category, which includes 2 ORs, the cell density was at its peak at 3 months and showed a significant decline only at the last time point tested: 24 months for MOR0-2 (Figure 2D) or 27 months for MOR267-16 (Figure 2E). In the third category, which contains 4 ORs (MOR13-4, MOR31-12, MOR122-1, and MOR279-2), the cell density increased from 3 months, reaching its peak at different time points (12 or 18 months), and displayed a significant decrease in later time points from the peak (Figure 2F–I).

Several findings emerged from the in situ hybridization data. First, the density of OSNs expressing individual ORs reached the maximum at different ages, ranging from 3 to 18 months. Second, the expression patterns of different ORs showed differential trajectories during aging. For some ORs, the cell density did not show a significant decline up to 24 months (Figure 2A–C,E). For others, a significant decline was observed at 24 months (Figure 2D,F–I). At 27 months, the decline became more evident in 2 of 3 ORs (Figure 2E,I). Third, there was no clear correlation between the expression pattern changes and the zonal distribution of OSNs expressing different ORs. All 3 categories described above contain one or more ORs expressed in zone 4. The data reveal that even though the cell loss is not uniform for different subtypes of OSNs, there is a significant age-related reduction of OSNs expressing certain ORs.

Odorant response properties of individual MOR23 cells in aged mice

We then tested the odorant sensitivity of individual sensory neurons in aged olfactory epithelia. Due to intermingling of OSNs expressing different ORs in the olfactory epithelium, we used a gene-targeted mouse line in which the OR MOR23 is genetically tagged by tauGFP allowing identification of these neurons (Vassalli et al. 2002). This line was chosen because an effective ligand (lyral) for this receptor has been identified (Touhara et al. 1999; Grosmaitre et al. 2006). MOR23 cells were distributed in zone 1 and readily visible in the intact epithelium (Figure 3A). To quantify the cell densities, we randomly took 47 and 29 images (222 × 168 μm) from 3-month-old mice (3 animals) and 24-month-old mice (5 animals), respectively. The averaged cell density per surface area decreased from 303.1 ± 12.3/mm^2 at 3 months to 167.7 ± 18.6/mm^2 at 24 months ($P < 0.0001$, *t*-test; Figure 3B). Two other 24 months mice examined had no green cells and thus were excluded from this analysis (potential reasons are discussed later). These data indicate that the MOR23 cell density decreased with age.

Our previous patch clamp recordings from 53 MOR23 cells obtained from 1-month to 3-month-old mice indicate that all MOR23 cells respond to lyral, but the response kinetics and sensitivity display individual variations to some extent (Grosmaitre et al. 2006). Using perforated patch clamp, here we compared the lyral-induced responses in the MOR23 cells from 3-month and 24-month-old mice (Figure 4A,B). Under voltage clamp mode, brief lyral puffs (at 10 μM) induced the inward transduction currents with different response kinetics in different cells (Figure 4A). Under current-clamp mode, the same lyral puffs depolarized the membrane potential and trigged action potentials (Figure 4B). To evaluate the sensitivity of OSNs from these 2 age groups, we obtained the dose–response relations in MOR23 cells from 3-month and 24-month-old mice. For each cell, 4 concentrations (10^{-7}, 10^{-6}, 10^{-5}, and 10^{-4} M) of lyral were sequentially applied from the lowest to highest with an interval of >1 min to minimize odorant adaptation. MOR23 cells responded to lyral in a dose-dependent manner, and the induced currents increased with concentration (Figure 4C–E). These concentrations were chosen because the dynamic range of MOR23 cells often covers 3–4 log units from a threshold around 10^{-7} M to a saturating response near 10^{-4} M (Grosmaitre et al. 2006). The normalized peak transduction current

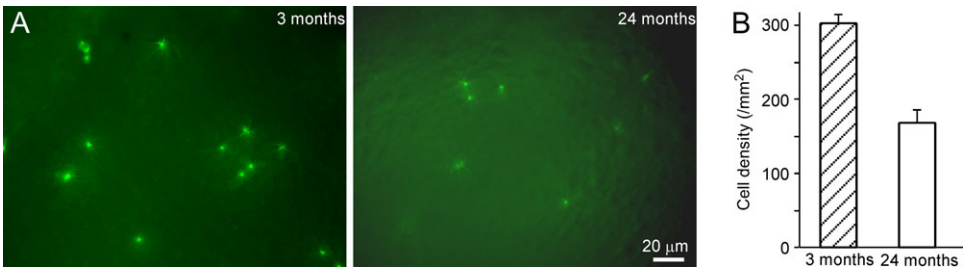

Figure 3 The surface density of MOR23-GFP cells decreases with age. **(A)** Two sample images were taken from the whole-mount olfactory epithelium at different ages: 3 months (left) or 24 months (right). Note that the MOR23 cells showed weaker GFP signals in the aged mice than young adults. **(B)** The density of MOR23 cells per surface area was averaged from 47 (3 months) and 29 (24 months) images. The difference between the 2 time points was significant (*t*-test, $P < 0.0001$).

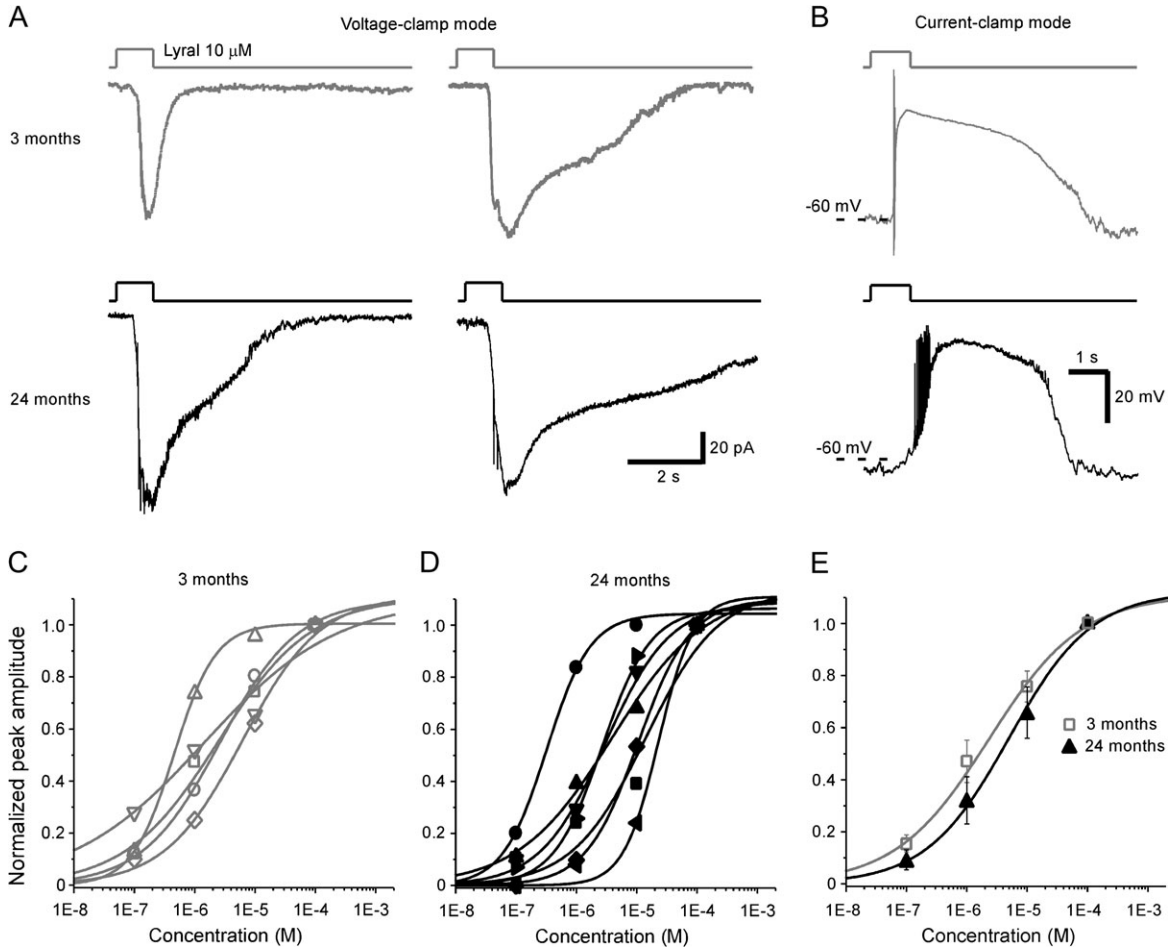

Figure 4 Individual MOR23 cells from aged mice show similar sensitivity and dose–response relations as those from younger counterparts. **(A)** Under voltage clamp mode, inward currents were elicited by lyral puffs in 4 MOR23 cells from different age groups: 2 from 3 months (upper panel in gray) and 2 from 24 months (lower panel in black). **(B)** Under current-clamp mode, lyral puffs induced the receptor potential and evoked action potentials in 2 MOR23 cells from different age groups: 3 months (upper panel in gray) or 24 months (lower panel in black). **(C, D)** Individual MOR23 cells from 3-month-old mice **(C)** and 24-month-old mice **(D)** were stimulated by lyral puffs at different concentrations (from 10^{-7} to 10^{-4} M) under voltage clamp mode. For each cell, the peak currents are normalized to that elicited by 10^{-4} M and plotted against the concentration. The dose–response curves are then fitted with the Hill equation. The holding potential was −65 mV for all cells. **(E)** The averaged dose–response curves are plotted for MOR23 cells from 3-month-old mice (n = 5 in C) and 24-month-old mice (n = 7 in D). Error bars = standard errors.

versus the concentration is plotted for each cell and fitted with the Hill equation, $I_{norm} = 1/(1 + (K_{1/2}/C)^n)$, where I_{norm} represents the peak current normalized to that induced by 10^{-4} M in that cell, $K_{1/2}$ the concentration at which half of the maximum response was reached, C the concentration of odorant, and n the Hill coefficient (Figure 4C,D). The maximum currents induced by 10^{-4} M lyral from the 3 months group range from 42 to 158 pA, $K_{1/2} = 2.6 \pm 1.0$ μM, and $n = 0.7 \pm 0.1$ (5 cells). The maximum currents from the 24 months group range from 58 to 292 pA, $K_{1/2} = 7.1 \pm 2.6$ μM, and $n = 1.0 \pm 0.1$ (7 cells). These data indicate different sensitivities among MOR23 cells from the same age group. Averaged dose–response curves from these 2 groups failed to show significant differences ($P > 0.05$ for both $K_{1/2}$ and the Hill coefficient, t-test; Figure 4E). The results suggest that individual sensory neurons in aged mice can be as sensitive as those from young adults.

Discussion

We investigated age-related alterations in the expression patterns of individual OR genes in the mouse olfactory epithelium using in situ hybridization. The results reveal a significant reduction of the cell densities for some ORs, but not for others until 24 months, indicating differential changes for different subtypes of OSNs during aging. Among the 3 ORs tested at 27 months, 2 showed significant reduction in cell densities from the peak. Using patch clamp recordings, we then examined the sensitivity of individual MOR23 cells in aged animals. Although the surface density

of MOR23 cells decreases from 3 to 24 months, the dose–response curves of single cells from aged mice cover a similar range as those from young counterparts. The data indicate that age-related cell loss in the olfactory epithelium is not uniform among OSNs expressing different ORs and individual OSNs can function relatively normally. The results suggest that the peripheral changes may not be sufficient to explain age-related smell loss, which likely involves central mechanisms in the brain.

Expression patterns of individual ORs in aged epithelium

The rodent olfactory epithelium shows significant signs of degenerative changes in aging, including a net loss of OSNs, which results in a thinner epithelium (Hinds and McNelly 1981; Loo et al. 1996; Rosli et al. 1999). However, it is not clear whether such loss is a direct consequence of aging or a result of age-related conditions (Rawson 2006). The fact that the anterior portion of the epithelium shows more damage than the posterior part suggests that the damage may result from cumulative environmental insults or in combination with age (Loo et al. 1996). In the better protected, posterior part of the olfactory epithelium, we here report differential changes in the cell densities of individual ORs in normal aging. For some ORs, a significant reduction in cell densities is evident at 24 months and becomes more profound at 27 months (Figure 2). The reduction in cell densities for most ORs will become more severe if the more damaged anterior part is included in this analysis. Although we cannot rule out the contributions of environmental factors, the fact that aged mice from different sources did not show systematic differences supports that aging per se plays a major role in our observation.

Our findings imply that the composition of OSNs expressing different ORs is dynamically regulated during aging. This is surprising given that these experimental mice are kept in similar environment. One possibility is that different ORs may have distinct functions throughout the lifespan. One can imagine that OSNs expressing ORs essential for suckling and mating behaviors tend to be lost during later ages. The results also raise the possibility that the environmental odors, which do not equally stimulate all ORs, may have an effect on the survival of certain subtypes of OSNs (see below).

In examining the density of MOR23 cells using whole-mount epithelia from zone 1 (Figure 3), we did not find green cells in two 24-month-old animals, which may result from several possibilities. First, the dorsal epithelium in these 2 animals might have more severe damage. There were large patches losing the characteristics of olfactory epithelium. Even in the areas that supporting cells were evident, there were fewer dendritic knobs. These changes may correspond to morphological alterations in the localized, degenerated olfactory epithelium reported in aged rodents (Breckenridge et al. 1997; Rosli et al. 1999). Alternatively, we might have lost most of the better preserved, posterior olfactory epithelium during dissection for these 2 mice. Second, we cannot completely rule out a possible infection, though it is unlikely because the animals were housed in a barrier-protected facility. Third, there is a chance that the MOR23 cells in these mice express GFP at a low level that falls below the detection threshold. In fact, the MOR23 cells from 3-month-old animals are brighter than those from 24-month-old animals. This may reflect a reduced expression level of MOR23 receptor in individual cells in aged animals or a reduction in GFP production. By excluding these mice from the analysis, we may have underestimated the overall reduction in the MOR23 cells during aging, but this should not affect the main conclusions drawn from these experiments.

Sensitivity of individual OSNs in aged mice

Compared with the well-documented morphological changes in the aging olfactory epithelium, few studies have examined odor-induced activity from aged rodents. In a senescence-accelerated mouse model, odor-induced electro-olfactogram (EOG) signals become smaller with age, accompanied by reduced olfactory sensitivity in behavioral tests (Nakayasu et al. 2000). In another study using voltage-sensitive dye imaging of the rat olfactory epithelium, odor-evoked activity in the middle and posterior zones fails to show age-related changes in the overall responses (Loo et al. 1996).

Instead of measuring the summated activity from populations of neurons in EOG or optical signals, we have examined the response properties from individual OSNs with a defined receptor (MOR23) by patch clamp recordings. Consistent with our previous findings, all MOR23 cells tested responded to lyral but with somewhat different kinetics and sensitivity (Grosmaitre et al. 2006). The difference is also evident among the cells obtained from animals at the same age (either 3 months or 24 months; Figure 4). The observed heterogeneity cannot be explained by uncontrollable, methodological factors because we monitored the leakage and ionic currents throughout the experiments and confirmed that they were similar in different cells. Several biological factors could potentially contribute to such heterogeneity within the same age group. Due to the asynchronous neurogenesis of OSNs, the age of the recorded cells can vary from a few days (just matured) to many months due to the continuous neurogenesis (Loo et al. 1996; Weiler and Farbman 1997). The lifespan of mature OSNs can be as long as 12 months in the absence of disease-associated destruction (Hinds et al. 1984). The range in the age of OSNs may affect their cellular properties, including the expression levels of MOR23 mRNA and protein and the signal transduction cascade involved in odor responses. Notably, the MOR23 cells from the aged mice displayed similar response amplitude and sensitivity as compared with those from younger adults. The study from MOR23 cells does not rule out the possibility that

some OSNs expressing other ORs may have decreased sensitivity. Nevertheless, these results indicate that individual olfactory neurons with unchanged sensitivity can still be found in aged animals.

Can age-related changes in the olfactory epithelium be reversible?

The current study reveals that aging does not cause a uniform loss of all subtypes of OSNs and their sensitivity, which implies that smell loss in aging might be a preventable and reversible process from the peripheral aspect. Several experimental manipulations can indeed affect the survival of OSNs. For instance, the open side of young mice subjected to neonatal naris closure shows loss of OSNs in patches of olfactory epithelium, especially in the anterior portion (Tian and Ma 2008a). Such damage becomes more severe with the animals' age and the length of closure (Maruniak et al. 1990), presumably due to the extra trauma caused to the open side that serves as the obligatory breather with doubled airflow. The aging olfactory epithelium displays similar pathological changes, which may result to some extent from cumulative insults to the olfactory system. In addition, neuronal activity (spontaneous or odor-induced) plays a role in the survival of OSNs in a competitive environment (Zhao and Reed 2001; Yu et al. 2004). One study demonstrates that odorant stimulation rescues populations of OSNs from apoptosis after bulbectomy (Watt et al. 2004). It would be interesting to know whether experimental manipulations (keeping the animals in a cleaner environment or long-term exposure to certain odors) can prevent the reduction of specific OSN populations.

Potential mechanisms of age-related smell loss

Age-related alterations in the central olfactory system have also been reported in the literature. The consequences of the observed reduction in the cell densities in the current study are yet to be determined. We have never observed a complete elimination of OSNs expressing a given OR up to 27 months in mice, suggesting that the total number of glomeruli should not be reduced by this age. For an individual glomerulus, the functional effects of a reduction in the number of convergent OSNs are not clear. An earlier study in aged rats indicates that the decline in the number of OSNs precedes the changes in the olfactory bulb, suggesting that atrophic changes in the olfactory bulb may be secondary to changes in the olfactory epithelium (Hinds and McNelly 1981). Age-related changes in the peripheral and central olfactory system may vary dramatically among different species. In humans, the number of glomeruli and mitral cells declines steadily with age at an approximate rate of 10% per decade from young adults (Meisami et al. 1998). Notably, there are also tremendous individual variations in the number of glomeruli (Maresh et al. 2008). The current study suggests that the peripheral alterations in the aged olfactory epithelium may not be sufficient to cause smell loss, which likely involves central changes in the brain.

Funding

National Institute on Deafness and Other Communication Disorders/National Institutes of Health (R01 DC006213 to M.M. and R03 DC008391 to X.G.); Institute on Aging at the University of Pennsylvania (to M.M.).

Supplementary material

Supplementary table 1 can be found at http://www.chemse.oxfordjournals.org/.

References

Breckenridge LJ, Cameron J, Puri N, Reid O, McGadey J, Smith RA. 1997. Localised degeneration occurs in aged mouse olfactory epithelium. J Anat. 191(Pt 1):151–154.

Chen Y, Getchell TV, Sparks DL, Getchell ML. 1993. Patterns of adrenergic and peptidergic innervation in human olfactory mucosa: age-related trends. J Comp Neurol. 334:104–116.

Conley DB, Robinson AM, Shinners MJ, Kern RC. 2003. Age-related olfactory dysfunction: cellular and molecular characterization in the rat. Am J Rhinol. 17:169–175.

Doty RL, Shaman P, Applebaum SL, Giberson R, Siksorski L, Rosenberg L. 1984. Smell identification ability: changes with age. Science. 226:1441–1443.

Enwere E, Shingo T, Gregg C, Fujikawa H, Ohta S, Weiss S. 2004. Aging results in reduced epidermal growth factor receptor signaling, diminished olfactory neurogenesis, and deficits in fine olfactory discrimination. J Neurosci. 24:8354–8365.

Firestein S. 2001. How the olfactory system makes sense of scents. Nature. 413:211–218.

Getchell TV, Peng X, Green CP, Stromberg AJ, Chen KC, Mattson MP, Getchell ML. 2004. In silico analysis of gene expression profiles in the olfactory mucosae of aging senescence-accelerated mice. J Neurosci Res. 77:430–452.

Grosmaitre X, Vassalli A, Mombaerts P, Shepherd GM, Ma M. 2006. Odorant responses of olfactory sensory neurons expressing the odorant receptor MOR23: a patch clamp analysis in gene-targeted mice. Proc Natl Acad Sci USA. 103:1970–1975.

Guillery RW. 2002. On counting and counting errors. J Comp Neurol. 447:1–7.

Hinds JW, Hinds PL, McNelly NA. 1984. An autoradiographic study of the mouse olfactory epithelium: evidence for long-lived receptors. Anat Rec. 210:375–383.

Hinds JW, McNelly NA. 1981. Aging in the rat olfactory system: correlation of changes in the olfactory epithelium and olfactory bulb. J Comp Neurol. 203:441–453.

Joly M, Deputte B, Verdier JM. 2006. Age effect on olfactory discrimination in a non-human primate, *Microcebus murinus*. Neurobiol Aging. 27:1045–1049.

Kern RC, Conley DB, Haines GK 3rd, Robinson AM. 2004. Pathology of the olfactory mucosa: implications for the treatment of olfactory dysfunction. Laryngoscope. 114:279–285.

Kraemer S, Apfelbach R. 2004. Olfactory sensitivity, learning and cognition in young adult and aged male Wistar rats. Physiol Behav. 81:435–442.

Lehrner JP, Gluck J, Laska M. 1999. Odor identification, consistency of label use, olfactory threshold and their relationships to odor memory over the human lifespan. Chem Senses. 24:337–346.

Loo AT, Youngentob SL, Kent PF, Schwob JE. 1996. The aging olfactory epithelium: neurogenesis, response to damage, and odorant-induced activity. Int J Dev Neurosci. 14:881–900.

Ma M. 2007. Encoding olfactory signals via multiple chemosensory systems. Crit Rev Biochem Mol Biol. 42:463–480.

Maresh A, Rodriguez Gil D, Whitman MC, Greer CA. 2008. Principles of glomerular organization in the human olfactory bulb—implications for odor processing. PLoS ONE. 3:e2640.

Maruniak JA, Henegar JR, Sweeney TP. 1990. Effects of long-term unilateral naris closure on the olfactory epithelia of adult mice. Brain Res. 526:65–72.

Meisami E, Mikhail L, Baim D, Bhatnagar KP. 1998. Human olfactory bulb: aging of glomeruli and mitral cells and a search for the accessory olfactory bulb. Ann N Y Acad Sci. 855:708–715.

Mombaerts P. 2006. Axonal wiring in the mouse olfactory system. Annu Rev Cell Dev Biol. 22:713–737.

Munger SD, Leinders-Zufall T, Zufall F. 2009. Subsystem organization of the mammalian sense of smell. Annu Rev Physiol. 71:115–140.

Murphy C, Schubert CR, Cruickshanks KJ, Klein BE, Klein R, Nondahl DM. 2002. Prevalence of olfactory impairment in older adults. JAMA. 288: 2307–2312.

Nakashima T, Kimmelman CP, Snow JB. 1984. Structure of human fetal and adult olfactory neuroepithelium. Arch Otolaryngol. 110:641–646.

Nakayasu C, Kanemura F, Hirano Y, Shimizu Y, Tonosaki K. 2000. Sensitivity of the olfactory sense declines with the aging in senescence-accelerated mouse (SAM-P1). Physiol Behav. 70:135–139.

Paik SI, Lehman MN, Seiden AM, Duncan HJ, Smith DV. 1992. Human olfactory biopsy. The influence of age and receptor distribution. Arch Otolaryngol. 118:731–738.

Rawson NE. 2006. Olfactory loss in aging. Sci Aging Knowledge Environ. 2006:pe6.

Rosli Y, Breckenridge LJ, Smith RA. 1999. An ultrastructural study of age-related changes in mouse olfactory epithelium. J Electron Microsc (Tokyo). 48:77–84.

Ship JA, Pearson JD, Cruise LJ, Brant LJ, Metter EJ. 1996. Longitudinal changes in smell identification. J Gerontol A Biol Sci Med Sci. 51: M86–M91.

Stevens JC, Cain WS. 1987. Old-age deficits in the sense of smell as gauged by thresholds, magnitude matching, and odor identification. Psychol Aging. 2:36–42.

Tian H, Ma M. 2008a. Activity plays a role in eliminating olfactory sensory neurons expressing multiple odorant receptors in the mouse septal organ. Mol Cell Neurosci. 38:484–488.

Tian H, Ma M. 2008b. Differential development of odorant receptor expression patterns in the olfactory epithelium: a quantitative analysis in the mouse septal organ. Dev Neurobiol. 68:476–486.

Touhara K, Sengoku S, Inaki K, Tsuboi A, Hirono J, Sato T, Sakano H, Haga T. 1999. Functional identification and reconstitution of an odorant receptor in single olfactory neurons. Proc Natl Acad Sci USA. 96:4040–4045.

Trojanowski JQ, Newman PD, Hill WD, Lee VM. 1991. Human olfactory epithelium in normal aging, Alzheimer's disease, and other neurodegenerative disorders. J Comp Neurol. 310:365–376.

Vassalli A, Rothman A, Feinstein P, Zapotocky M, Mombaerts P. 2002. Minigenes impart odorant receptor-specific axon guidance in the olfactory bulb. Neuron. 35:681–696.

Watt WC, Sakano H, Lee ZY, Reusch JE, Trinh K, Storm DR. 2004. Odorant stimulation enhances survival of olfactory sensory neurons via MAPK and CREB. Neuron. 41:955–967.

Weiler E, Farbman AI. 1997. Proliferation in the rat olfactory epithelium: age-dependent changes. J Neurosci. 17:3610–3622.

Wysocki CJ, Gilbert AN. 1989. National Geographic Smell Survey. Effects of age are heterogenous. Ann N Y Acad Sci. 561:12–28.

Yu CR, Power J, Barnea G, O'Donnell S, Brown HE, Osborne J, Axel R, Gogos JA. 2004. Spontaneous neural activity is required for the establishment and maintenance of the olfactory sensory map. Neuron. 42:553–566.

Zhao H, Reed RR. 2001. X inactivation of the OCNC1 channel gene reveals a role for activity-dependent competition in the olfactory system. Cell. 104:651–660.

Accepted August 17, 2009